MdERDL6-mediated glucose efflux to the cytosol promotes sugar accumulation in the vacuole through up-regulating TSTs in apple and tomato

Lingcheng Zhu[a], Baiyun Li[a], Limin Wu[b], Huixia Li[a], Zhengyang Wang[a], Xiaoyu Wei[a], Baiquan Ma[a], Yanfeng Zhang[c], Fengwang Ma[a,1], Yong-Ling Ruan[d,1], and Mingjun Li[a,1]

[a]State Key Laboratory of Crop Stress Biology in Arid Areas/Shaanxi Key Laboratory of Apple, College of Horticulture, Northwest A&F University, Yangling, Shaanxi, 712100, China; [b]Agriculture and Food, Commonwealth Scientific and Industrial Research Organisation, Canberra, ACT 2601, Australia; [c]Hybrid Rapeseed Research Center of Shaanxi Province, Yangling, Shaanxi, 712100, China; and [d]School of Environmental and Life Sciences, The University of Newcastle, Callaghan, NSW 2308, Australia

Edited by Natasha V. Raikhel, Center for Plant Cell Biology, Riverside, CA, and approved November 17, 2020 (received for review November 11, 2020)

Sugar transport across tonoplasts is essential for maintaining cellular sugar homeostasis and metabolic balance in plant cells. It remains unclear, however, how this process is regulated among different classes of sugar transporters. Here, we identified a tonoplast H^+/glucose symporter, MdERDL6-1, from apples, which was highly expressed in fruits and exhibited expression patterns similar to those of the tonoplast H^+/sugar antiporters MdTST1 and MdTST2. Overexpression of *MdERDL6-1* unexpectedly increased not only glucose (Glc) concentration but also that of fructose (Fru) and sucrose (Suc) in transgenic apple and tomato leaves and fruits. RNA sequencing (RNA-seq) and expression analyses showed an up-regulation of *TST1* and *TST2* in the transgenic apple and tomato lines overexpressing *MdERDL6-1*. Further studies established that the increased sugar concentration in the transgenic lines correlated with up-regulation of *TST1* and *TST2* expression. Suppression or knockout of *SlTST1* and *SlTST2* in the *MdERDL6-1*–overexpressed tomato background reduced or abolished the positive effect of *MdERDL6-1* on sugar accumulation, respectively. The findings demonstrate a regulation of *TST1* and *TST2* by *MdERDL6-1*, in which Glc exported by MdERDL6-1 from vacuole up-regulates *TST1* and *TST2* to import sugars from cytosol to vacuole for accumulation to high concentrations. The results provide insight into the regulatory mechanism of sugar accumulation in vacuoles mediated by the coordinated action of two classes of tonoplast sugar transporters.

cytosolic sugar signaling | H^+/glucose symporter | H^+/sugar antiporter | intracellular communication | sugar transport

Soluble sugars play important roles not only as nutrients but also as signal molecules in plant growth and development (1). In fleshy fruits, sucrose (Suc) and monosaccharides (glucose [Glc] and fructose [Fru]) are also central to fruit quality as they are the main nutrients and sweetening compounds. The distribution of sugars in plant cells is dependent on several transport steps across cell membranes in addition to long-distance translocation through the phloem (2).

In most plants, Suc is transported from photosynthetically active leaves (source), through the phloem, to nonphotosynthetic sink organs, such as fruits, roots, and stems. Suc is then either directly transported into sink cells or taken up in the form of hexoses (Glc and Fru) after cleavage by an extracellular invertase (3, 4). Within the sink cells, soluble sugars are first metabolized to meet the requirements for energy and carbon skeleton production. Excessive sugars are generally converted into starch for storage in the plastid or imported into vacuoles for transient or long-term storage mediated by vacuolar sugar transporters (2, 5). The vacuole occupies up to 90% of the cell volume, where most sugars are compartmentalized, typically in the parenchyma cells of many sugar-accumulating organs such as sugar cane stems, sugar beet roots, and fresh fruits of tomato, apple, and orange (5–7). While considerable effort has been made to understand sugar transport and accumulation in plants, our knowledge of the mechanism by which cells accumulate high concentrations of sugars in the vacuole remains rather limited.

Sugar input into vacuoles is largely determined by different classes of sugar transporters located on the tonoplast (6). The tonoplast monosaccharide transporter (TMT), now renamed as tonoplast sugar transporter (TST), and the vacuolar glucose transporter (vGT) families encode proteins to mediate sugar influx into vacuoles as H^+/sugar antiporters (8–10). In *Arabidopsis*, AtvGT1 is a tonoplast transporter specific for Glc with a role in seed germination and flowering (10), while *AtTMT1/2* exhibits a broad substrate specificity and could transport Glc, Fru, and Suc into the vacuole (8, 11). More recently, SWEETs (sugars will eventually be exported transporters) have been identified as energy independent uniporters from *Arabidopsis*, rice, and other species, mediating concentration-dependent sugar influx or efflux across membranes (12). In the SWEET family of *Arabidopsis*, AtSWEET16 and AtSWEET17 were localized on the tonoplasts of root and leaf cells, where the former transported Suc, Glc, and Fru (13), while the latter appeared specific to Fru (14).

Among the transporters that had been identified, only one member from the TST subfamily, namely, the TST2 subfamily, has been shown to play important roles in sugar accumulation (9, 15, 16). TSTs from different plants displayed different substrate

Significance

Sugar transport across membranes is essential for maintaining cellular sugar homeostasis and metabolic balance in plant cells. However, it remains unclear how this process is regulated among different classes of sugar transporters. Here, we identified an apple tonoplast H^+/glucose symporter, MdERDL6-1, that exports glucose to cytosols to up-regulate the expression of H^+/sugar antiporter genes *TST1* and *TST2* to import sugars from cytosol to vacuole for accumulation to high concentrations in apples and tomatoes. The findings provide insights into the regulatory mechanism underlying sugar exchange between cytosol and vacuole.

Author contributions: L.Z., F.M., Y.-L.R., and M.L. designed research; L.Z., B.L., H.L., Z.W., and X.W. performed research; L.Z., L.W., B.M., Y.Z., Y.-L.R., and M.L. analyzed data; L.Z., Y.-L.R., and M.L. wrote the paper; and F.M., Y.-L.R., and M.L. supervised research.

The authors declare no competing interest.

This article is a PNAS Direct Submission.

[1]To whom correspondence may be addressed. Email: limingjun@nwsuaf.edu.cn, yongling.ruan@newcastle.edu.au, or fwm64@nwsuaf.edu.cn.

This article contains supporting information online at https://www.pnas.org/lookup/suppl/doi:10.1073/pnas.2022788118/-/DCSupplemental.

Published December 21, 2020.

specificities. For example, the watermelon ClTST2 protein exhibited similar transport activity for Suc, Fru, and Glc (16), while the BvTST2.1 protein from sugar beets has a specific affinity for Suc and is responsible for Suc accumulation in the taproots (9).

Apart from the H^+/sugar antiporter, TSTs, two types of H^+/sugar symporters, the Suc exporter SUC4 (17) and the Glc exporter early response to dehydration like 6 (ERDL6), have also been identified to function on the tonoplast (18, 19). The operation of H^+-coupled importers (e.g., TSTs, as an antiporter) and exporters (e.g., SUC4 and ERDL6, as symporters) on the tonoplast regulates sugar homeostasis between vacuole and cytoplasm (6). In *Arabidopsis*, *AtSUC4* is weakly expressed in Suc-accumulating leaf mesophyll cells, and high SUC4 activity is unfavorable for sugar accumulation (17). It was reported that AtERDL6 acts as a Glc exporter in *Arabidopsis* to transfer Glc from the vacuole to the cytosol, as indicated by the finding that the corresponding *erdl6* mutant accumulated more Glc in the vacuole (18, 19).

It is noteworthy that orthologous genes of *AtERDL6* exhibited higher expression levels in a wide range of sugar-accumulating fleshy fruits, such as those from pineapples (20), tomatoes (21), oranges (22), and apples (23, 24). The expression level of these *ERDL6* orthologs genes generally matches with the fruit sugar content. In apples, the mRNA level and protein abundance of multiple *MdERDL6* family members were strongly and positively correlated with Suc and Fru concentrations in the fruits, in parallel to high expression of *MdTST1/2* (23, 24). The high expression of *MdERDL6* genes in the sugary apple fruits is intriguing given that ERDL6 is an exporter of Glc from vacuoles and its overexpression in *Arabidopsis* impaired cold tolerance and seed germination (19). It remains unknown if ERDL6s contribute to sugar accumulation in fruits and, in particular, how ERDL6s and TSTs may coregulate sugar levels in the vacuoles.

To explore the potential roles and cross talks of tonoplast H^+/sugar symporters and antiporters in sugar accumulation, we first characterized *MdERDL6-1* expression patterns and the transport activities of the encoded protein. This was followed by overexpression of *MdERDL6-1* in apple and tomato (*Solanum lycopersicum* cv. Micro-Tom). The data obtained indicated that MdERDL6-1 functions as a H^+/Glc symporter on the tonoplast to export Glc from the vacuole into the cytosol. Overexpression of *MdERDL6-1* in apples and tomatoes substantially increased Glc, Fru, and Suc concentrations in leaves and fruits. This promoting effect was owing to the increased expression of *TST1* and *TST2* in the transgenic lines because the positive effect of *MdERDL6-1* overexpression on sugar level was abolished or reduced once *TST1* and *TST2* were knocked out or suppressed, respectively. Overall, these results, together with other findings documented in this paper, identified a tonoplast H^+/Glc symporter from apple that exports Glc from vacuoles and established that the increased Glc efflux mediated by MdERDL6-1 into the cytosol up-regulated *TST1* and *TST2* expression to promote sugar import into the vacuoles. The findings provide insights into the regulatory mechanism on sugar transport between cytosol and vacuole across tonoplast and offer potential opportunities to improve fruit sugar levels, hence fruit quality and yield.

Results

***MdERDL6* Expression in Apples and the Subcellular Localization of Its Encoded Protein.** To identify major energy-dependent sugar transporters operating on tonoplast in apple, the AtERDL6, AtTST, or AtvGT protein sequences were used as queries to search *Malus* × *domestica* genome GDDH13 v1.1 (25). The exercise identified 11 *MdERDL6s*, six *MdTSTs,* and three *MdvGTs* genes from the updated *Malus* × *domestica* genome. Phylogenetic analysis revealed that the 11 candidate *MdERDL6s* could be divided into three groups. Among them, *MdERDL6-1* and *MdERDL6-2* were clustered with *AtERDL6*, *AtERDL6-5,* and *BvIMP* (an *AtERDL6* ortholog from sugar beet) (*SI Appendix*, Fig. S1), all of which function as H^+/Glc symporters in *Arabidopsis* (18, 19). The identified *MdTST1*, *2*, and *3* were all orthologous to *AtTMT2* (*SI Appendix*, Fig. S1).

Transcriptional patterns of *MdERDL6s*, *MdTSTs,* and *MdvGTs* were analyzed in developing fruit and other tissues, including shoot tips and mature leaves based on our RNA sequencing (RNA-seq) data (Fig. 1*A* and Dataset S1*A*). Six of the 11 *MdERDL6* orthologs (from *MdERDL6-1* to *MdERDL6-6*), along with *MdTST1* and *MdTST2,* exhibited an increased expression as fruit develops, which correlated with fruit Fru and Suc levels (Fig. 1*A*). Among the 11 *MdERDL6* genes, *MdERDL6-1* exhibited a higher expression level in developing fruit based on the reads per kilobase per million mapped reads (RPKM) values (Dataset S1*A*). qRT-PCR analyses also confirmed that *MdERDL6-1* was highly expressed in fruits, with a trend similar to those of *MdTST1* and *MdTST2* (Fig. 1*B*), implying a potential link between the *MdERDL6-1* and *MdTST1/2*. Thus, *MdERDL6-1* was selected as a candidate gene for further studies on its role in sugar accumulation and to test whether there is a functional coupling with *MdTST1* and *2*.

To determine the subcellular localization of MdERDL6-1, we transiently expressed a green fluorescent protein (GFP)-fused MdERDL6-1 protein in protoplasts, isolated from *Arabidopsis*, tobacco leaves, and apple calli. The *Arabidopsis* protoplast displayed red auto-fluorescence from chlorophyll outside the MdERDL6-1-GFP signal, with the latter colocalized with the tonoplast marker, VAC-RK (*SI Appendix*, Fig. S2). A clearer localization pattern was observed from tobacco protoplasts lysed by a mild osmotic shock, where MdERDL6-1-GFP fluorescence was seen only in the membrane of the vacuoles with the auto-fluorescent chloroplasts sitting outside (Fig. 2*A*). Further, the MdERDL6-1-GFP fluorescence was localized on membranes inside the plasma membranes of protoplasts from apple calli cells (Fig. 2*B*). These data collectively indicate that MdERDL6-1 targets to tonoplast in vivo.

Functional Characterization of MdERDL6-1 in Yeast. To characterize the transport properties of MdERDL6-1 protein, we cloned *MdERDL6-1* into the vector pYES-DEST2-eGFP and expressed it in a yeast mutant deficient in hexose transport, which grows only on maltose (26). Analysis of the transformed yeast lines by fluorescent microscopy revealed that the MdERDL6-1-GFP fluorescence clearly localized to the plasma membrane but not to the internal compartments of yeast cells (Fig. 2*C*), consistent with a previous report that the tonoplast gene *AtERDL10* from *Arabidopsis* was also targeted to the plasma membrane in the yeast (19). These observations indicate that the yeast system could be used to detect the transport properties of MdERDL6-1 protein.

We then cloned *MdERDL6-1* into the vector pYES-DEST2, in both the sense and antisense orientation, and expressed them in the yeast mutant EBY.VW4000. The yeast transformed with pYES-DEST2-MdERDL6-1 in the sense orientation was used to assess complementation efficiency, with those transformed with *MdERDL6-1* in the antisense orientation serving as the control. As expected, expression of *MdERDL6-1* in the antisense orientation in this null mutant did not restore growth on sugar-containing medium. By contrast, the strain expressing *MdERDL6-1* in the sense orientation regained the capacity to grow well on 2% Glc-containing medium but could not grow on medium containing Fru, galactose (Gal), or xylose (Xyl) (Fig. 2*D*). This indicates that MdERDL6-1 functions to specifically transport Glc into the cytosol of the yeast cells, thereby restoring the growth of the mutant. This notion was supported by ^{14}C-labeled D-hexose transport assay, which showed the transport capacity by MdERDL6-1 was clearly specific to Glc as compared with Fru and Gal (Fig. 2 *E* and *F*). The K_m of MdERDL6-1 for Glc was measured to be ~21.7 mM (Fig. 2 *E*,

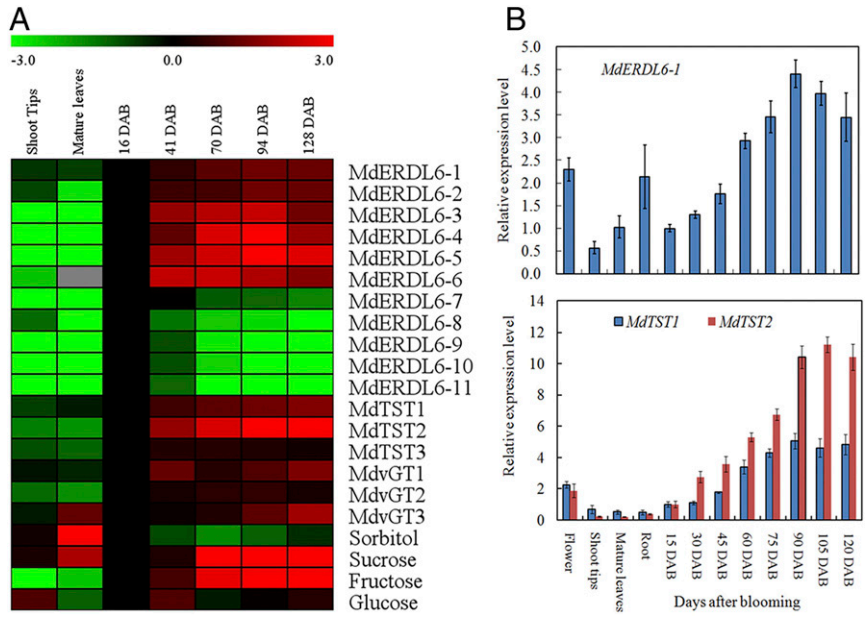

Fig. 1. The expression profiles of vacuolar sugar transporter genes, including *MdERDL6s*, *MdTSTs*, and *MdvGTs*, in apples. (*A*) A heat map of gene expression levels based on RNA-seq and sugar concentrations in different tissues including developing fruit. RPKM values measured with RNA-seq are shown in Dataset S1*A*. Fold difference is designated as a log2 value, with the data in young fruit at 16 DAB set as 1. (*B*) Relative transcript levels of *MdERDL6-1*, *MdTST1*, and *MdTST2* in different tissues, including developing fruits based on qRT-PCR. For each sample, transcript levels were normalized with those of *MdActin*. Relative expression levels for each gene were obtained via the ddCT method, setting its expression in young fruit at 15 DAB as 1. The bars represent the mean value ± SD ($n \geq 3$).

Inset). Moreover, application of a proton uncoupler, carbonyl cyanide 3-chlorophenylhydrazone (CCCP), significantly decreased Glc uptake (Fig. 2*F*), suggesting that sugar uptake via MdERDL6-1 is probably driven by a proton gradient across the membrane. Taken together, the data from the heterologous expression analyses in yeast suggests that MdERDL6-1 acts as a H^+/Glc symporter.

Silencing *MdERDL6-1* Increased Glc Concentration, Whereas Its Overexpression Significantly Elevated Glc, Fru, and Suc Levels in the Apple Fruit Calli. To determine the role of *MdERDL6-1* in sugar accumulation, we first constructed RNA interference (RNAi) and overexpression vectors and transformed both into the cultured calli derived from apple fruit. The fruit calli is a fast-tracking efficient system to assess the function of genes related to fruit metabolism in apples (27, 28). After evaluation by using qRT-PCR, we obtained two silencing (SL1 and SL3) and two overexpression lines (OL3 and OL6) in which the *MdERDL6-1* expression was reduced to less than 30% of the wild-type (WT) level, but increased by more than 15 times relative to that in the WT, respectively (Fig. 3*A*). The growth rate of the fruit calli was clearly inhibited or increased in the silencing or the overexpression lines, respectively (Fig. 3*B*). Consistent with the finding that *MdERDL6-1* encoded a tonoplast-localized Glc exporter (Fig. 2), silencing *MdERDL6-1* increased Glc concentration by ~2 times, with Fru, Suc, and Sor levels remained unchanged (Fig. 3 *C* and *D*). Surprisingly, however, overexpressing *MdERDL6-1* did not lead to an expected reduction in Glc level, but rather doubled the concentrations of Glc and Fru, and increased Suc level by about 70 to 80% in the fruit calli on the 3% Glc- or Suc-containing medium (Fig. 3 *C* and *D*).

***In planta* Overexpression of *MdERDL6-1* in Apples and Tomatoes Also Substantially Increased Sugar Concentrations.** To further determine the impact of increases in *MdERDL6-1* expression on sugar accumulation *in planta*, we generated stable transgenic apple and tomato lines overexpressing *MdERDL6-1* driven by the CaMV35S promoter. Following PCR and qRT-PCR screening, as well as Western blotting detection using a specific antibody against MdERDL6-1, three transgenic apple lines (OEm-1, OEm-3, and OEm-4) and two tomato lines (OEs-1 and OEs-2) were obtained (*SI Appendix*, Fig. S3). The specificity of the antibody was indicated by the detection of a single band at the predicted size of MdERDL6-1 protein on Western blots loaded with proteins from apple leaves and tomato fruits (*SI Appendix*, Fig. S4). In the apple lines, the mRNA level of the *MdERDL6-1* was increased 5 to 10 times in leaves (*SI Appendix*, Fig. S3*C*) without affecting the transcript levels of other *MdERDL6* family members (*SI Appendix*, Fig. S5) or the growth and photosynthesis rates of the transgenic seedlings (Fig. 4*A* and *SI Appendix*, Fig. S6). The transgenic tomato plants showed expression of *MdERDL6-1* mRNA and protein in ripening fruits (*SI Appendix*, Figs. S3 *F* and *G* and S4), increased plant height and fruit size with delayed flowering, and reduced seed and fruit number (*SI Appendix*, Fig. S3*E* and Table S2).

To gain a clue as whether the overexpression of *MdERDL6-1* altered the subcellular sugar levels, we measured the expression of the sugar-sensitive reporter gene chlorophyll a/b binding protein (*CAB1*) in the transgenic lines. The transcription of *CAB1*, encoding the chlorophyll a/b binding protein 1, is negatively controlled by the cytosolic Glc concentration (19, 29). The analyses revealed that *CAB1* mRNA level was reduced by about 50 to 60% in the transgenic apple leaves and 40 to 50% in the tomato leaves and fruits overexpressing *MdERDL6-1* (*SI Appendix*, Fig. S7), indicating enhanced Glc export from vacuole into cytosol in the transgenic lines.

Since it takes ~5 y for any transformed apple plantlets to reach the adult reproductive phase for fruiting, we analyzed sugar levels in the leaves of transgenic apple seedlings. The assay revealed massive increases in the soluble sugar and starch levels, where the Glc content was increased by 3.9 to 4.5 times, while the Fru and Suc levels have risen by 6.9 to 8.0 times and 1.7 to 1.9 times of that in the WT, respectively (Fig. 4*A*). Similar results were observed in the leaves of two transgenic tomato lines

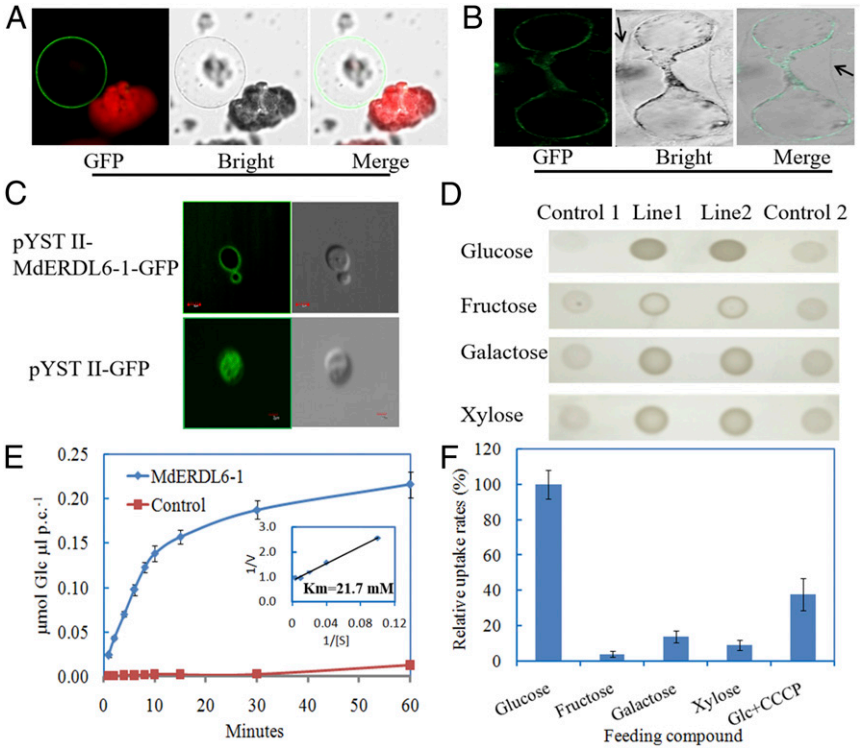

Fig. 2. Tonoplast localization of MdERDL6-1 in tobacco leaves and apple calli and its transport prosperities. (*A* and *B*) Tonoplast localization of the MdERDL6-1-GFP fusion protein in the isolated vacuoles of protoplasts from tobacco leaves (*A*) and the protoplasts from apple calli (*B*). The green fluorescence represents MdERDL6-1-GFP fusion proteins. Note the chloroplasts showing red auto fluorescence are located outside the ring of GFP fluorescence (*A*). For the apple calli protoplast (*B*), the MdERDL6-1-GFP fluorescence exhibited a ring-like pattern inside the plasma membrane (black arrows), indicating that MdERDL6-1 is localized to the tonoplast. (*C*) The localization of MdERDL6-1 to plasma membrane in yeast, based on MdERDL6-1-GFP fusion expression, in comparison with that of pYST II-GFP control in the yeast mutant strain EBY.VW4000. (Scale bars = 2 μm.) (*D*) Growth of the yeast mutant strain EBY.VW4000 expressing MdERDL6-1 on culture medium with 2% of different sugars. The deficient yeast mutant carrying the empty pYST II vector (Control 1) or the MdERDL6-1-antisense recombinant plasmid (Control 2) could not grow normally on each monosaccharide culture medium, whereas the yeast mutant transformed with MdERDL6-1-sense construct grew normally on glucose but slowly on Fru, Gal, and Xyl. (*E*) The transport capacity of [^{14}C] glucose was measured in yeast cells expressing MdERDL6-1 cDNA in the sense orientation (strain EBY.VW4000; blue circles) or the empty vector on 100 mM of glucose at pH 5.5. (*Inset*) The uptake rates with increasing concentrations of [^{14}C] glucose were determined 2 min after substrate addition and used to calculate the K_m value. The plot of a typical K_m determination is presented with five independent measurements. Here, a K_m value of 21.7 mM and a maximum uptake rate (V max) of 1.214 mmol · h^{-1} · ml^{-1} packed cells were determined for Glc uptake, driven by the MdERDL6-1 transporter. (*F*) Relative uptake rates of sugars at an initial concentration of 100 mM and the influence on glucose uptake by 50 μM uncoupler CCCP in MdERDL6-1–expressing yeast cells. Data represent average values of five independent transport tests (mean ± SD).

(*SI Appendix*, Fig. S8). Strikingly, we distinctly smelled a sweet aroma from the tomato fruit expressing *MdERDL6-1*, and indeed, the total soluble sugar content in the mature tomato fruit was 1.6 times of that in the WT. Consistently, the concentrations of Glc and Fru were increased by 60 to 95%, with Suc levels being more than doubled in the transgenic tomato fruits as compared to that of the WT (Fig. 4*B*).

***TST1* and *TST2* Were Up-Regulated in the *MdERDL6-1* Overexpressing Lines.** To explore the basis for the significant increase in the sugar levels in *MdERDL6-1* overexpressing plants, RNA-seq was performed to examine the changes in gene expression in the leaves of *MdERDL6-1* overexpressing apple lines, OEm-1 and 3. A total of 2,777 and 3,753 genes (log2 fold changes greater than 1, *P* value <0.01) were differentially expressed in the OEm-1 and OEm-3 lines, respectively, compared to the WT. Of these differentially expressed genes (DEGs), 2,631 genes were found in both lines (*SI Appendix*, Fig. S9, and Dataset S2*A*).

For the DEGs, the *MdERDL6-1* expression levels in OEm-1 and OEm-3 were 4.9 and 10.1 times, respectively, of that in the WT, while other *MdERDL6* orthologs remained unchanged, as confirmed by qRT-PCR (Fig. 5 *A* and *B* and *SI Appendix*, Fig. S5). The expression levels of three *MdCAB1s* were significantly decreased in the OEm-1 and OEm-3 lines (Fig. 5*B*). These expression results from RNA-seq were in agreement with those measured by using qRT-PCR (*SI Appendix*, Fig. S7), indicating that the RNA-seq data were credible. After annotation, 39 DEGs were found to relate carbohydrate metabolism and transport. Among them, 23 were down-regulated, including three beta-amylase genes (*MdBMYs*), five sorbitol transporter genes (*MdSOTs*), three hexose transporter genes (*MdHTs*), two *MdSWEET2s*, and seven genes related to Suc degradation (*MdCWINVs*, *MdNINVs*, *MdvAINVs*, and *MdSUSYs*), whereas ADP-glucose pyrophosphorylase genes (*MdAPLs*), chloroplast beta-amylase genes (*MdBMY3*), three fructokinase genes (*MdFRKs*), and two tonoplast sugar transporter genes (*MdTST1* and *MdTST2*) were up-regulated in both transgenic lines (Fig. 5*A*).

Among these DEGs, TSTs are tonoplast H^+/sugar antiporters and known to play an important role in the import of sugars to the vacuoles for storage (8, 9, 15, 16). Thus, we further examined *MdTST1* and *MdTST2* expression levels in all of the *MdERDL6-1* transgenic lines by using qRT-PCR and Western blotting. The mRNA expression levels of *MdTST1* and *MdTST2* were significantly up-regulated in the three apple overexpression lines (Fig. 5*D*), leading to increased protein levels by 2.2- to 3.3-fold as compared to that in the WT (Fig. 5*E* and *SI Appendix*, Fig. S4).

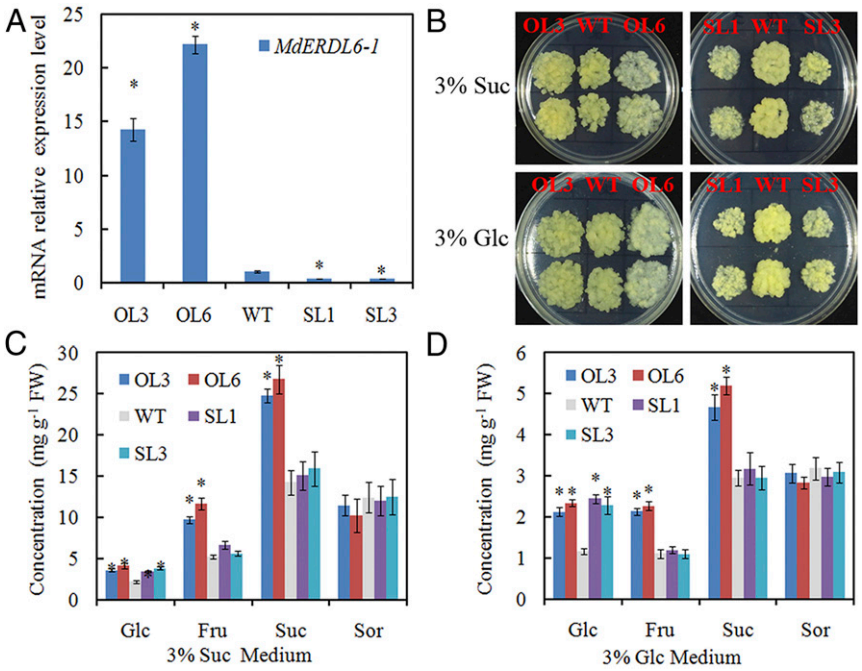

Fig. 3. The impact of altering *MdERDL6-1* expression on sugar (Glc, Fru, Suc, and Sor) concentrations in apple fruit calli. (*A*) *MdERDL6-1* expression levels in the overexpressing (OL3 and OL6) and silencing (SL1 and SL3) calli lines were measured by using qRT-PCR. The transcript levels were normalized to those of *MdActin*. The relative expression level for *MdERDL6-1* was obtained via the ddCT method, setting its expression in WT as 1. (*B*) The growth of the transformed calli on 3% Suc or 3% Glc medium. (*C* and *D*) The sugar concentrations of the transformed calli lines cultured on 3% Suc (*C*) or 3% Glc (*D*) medium. The bars represent the mean value ± SD ($n \geq 4$). *$P \leq 0.05$, a significant difference from the WT.

Similarly, in tomato fruit, the heterologous expression of *MdERDL6-1* also resulted in massive increases in *SlTST1* and *SlTST2* mRNA levels (Fig. 5*F*), resulting in an increase in their protein abundance by 2.7- to 4.0-fold (Fig. 5*G* and *SI Appendix*, Fig. S4).

***MdTST1* and *MdTST2* Expression Were Induced by Sugar-Feeding and Activated by *MdERDL6-1* Coexpression.** As shown above, *MdTST1* and *MdTST2* exhibited expression patterns that were similar to those of *MdERDL6-1* and correlated with sugar concentrations in leaves and fruits. Given that MdERDL6-1 was characterized as a tonoplast H^+/Glc symporter (Fig. 2) and *MdTST* orthologous genes *AtTMT1* and *2* were strongly induced by Glc (8), it raised the possibility that sugar exported by *MdERDL6-1* may up-regulate the expression of *MdTST1* and *MdTST2*. As the first step to test this hypothesis, the apple leaves were fed with different sugars, followed by qRT-PCR measurement of the respective

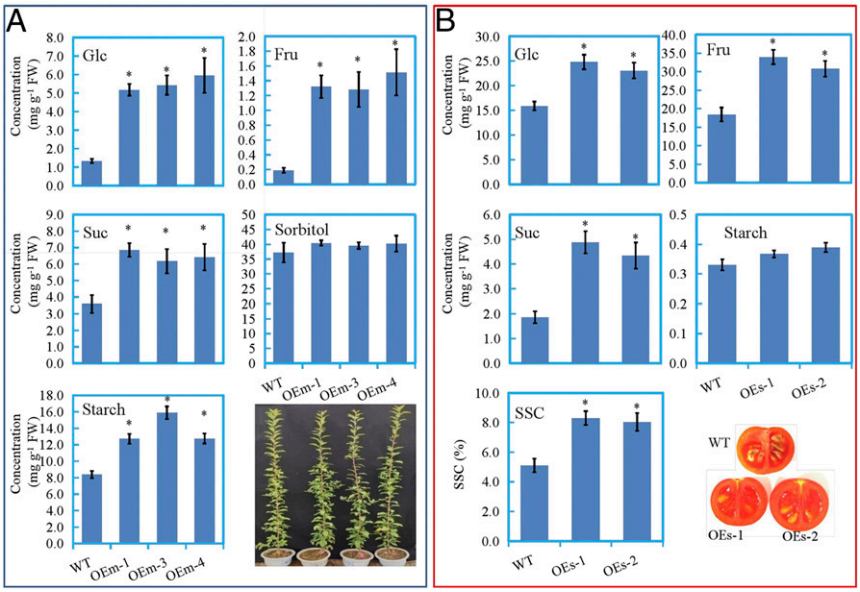

Fig. 4. The carbohydrate levels of the transgenic apple (OEm-1, OEm-3, and OEm-4) leaves and tomato (OEs-1 and OEs-2) fruits overexpressing *MdERDL6-1*. (*A*) Glc, Fru, Suc, Sor, and starch levels in mature leaves of transgenic apple. (*B*) The carbohydrate levels and soluble solids content in ripening fruits of transgenic tomato and longitudinal sections of the fruits. The bars represent the mean value ± SD ($n \geq 4$). *$P \leq 0.05$, a significant difference from the WT.

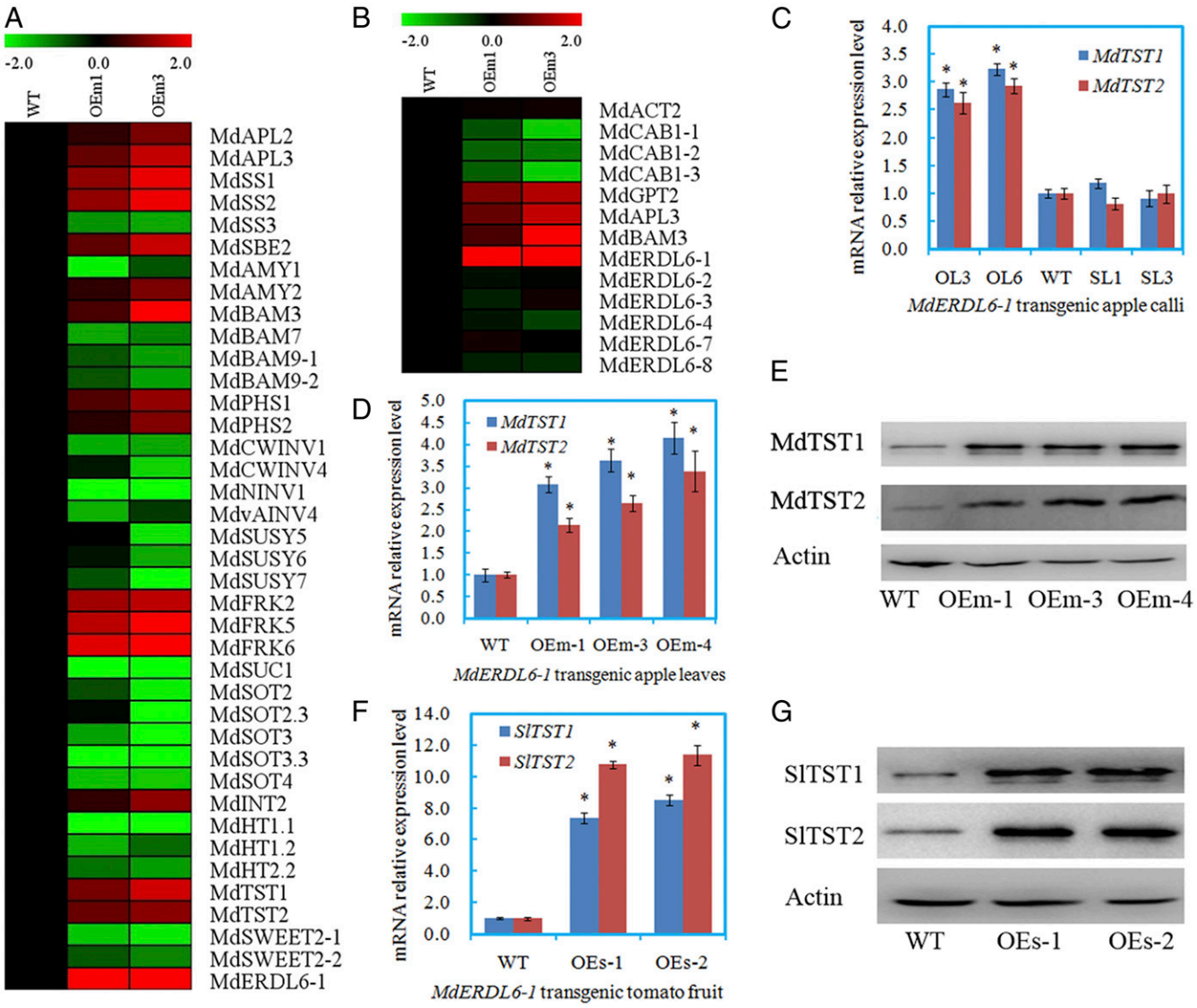

Fig. 5. The expression of genes related to carbohydrate metabolism and transport in the transgenic apple or tomato lines overexpressing *MdERDL6-1*. (*A*) A heat map illustrating different expression genes related to carbohydrate metabolism and transport in the leaves of transgenic apple lines (OEm-1 and OEm-3) based on RNA-seq. APL, ADP-glucose pyrophosphorylase; SS, starch synthase; SBE, starch branching enzyme; AMY, α-amylase; BMY, β-amylase; PHS, α-glucan phosphorylase; CWINV, cell wall invertase; NINV, neutral invertase; vAINV, vacuolar acid invertase; SUSY, sucrose synthase; FRK, fructokinse; SUC, sucrose transporter; SOT, sorbitol transporter; INT, inositol transporter; HT, hexose transporter; TST, tonoplast sugar transporter; SWEET, sugars will eventually be exported transporter; ERDL6, early response to dehydration like six. (*B*) A heat map illustrating the expression of marker genes involved in sugar response and other members of *MdERDL6* family in the leaves of transgenic lines based on RNA-seq. RPKM values measured with RNA-seq are shown in Dataset S2 *B* and *C*, respectively. The fold difference is designated as a log2 value, while the data in WT was set as 1 for each gene. ACT, actin; CAB, chlorophyll a/b binding protein; GPT, glucose-6-phosphate transporter. (*C*) Expression levels of *MdTST1* and *MdTST2* mRNAs in the transgenic apple calli overexpressing *MdERDL6-1* (OL3, 6) in comparison with the WT and two silencing lines (SL1, 3). (*D* and *E*) The expression levels of *MdTST1* and *MdTST2* mRNAs (*D*) and proteins (*E*) in the transgenic apple (OEm-1, OEm-3, and OEm-4) leaves overexpressing *MdERDL6-1*. (*F* and *G*) The expression levels of *SlTST1* and *SlTST2* mRNAs (*F*) and proteins (*G*) in the ripening fruits of transgenic tomato (OEs-1 and OEs-2) overexpressing *MdERDL6-1*. For qRT-PCR, the transcript levels were normalized to those of *MdActin* (*D*) and *SlActin* (*F*), respectively. Relative expression levels for each gene were obtained via the ddCT method, with its expression in WT set as 1. The bars represent the mean value ± SD ($n \geq 3$). *$P \leq 0.05$, a significant difference from the WT.

transcripts. In apple and tomato leaves, the mRNA levels of *MdTST1* and *2* and *SlTST1* and *2* were significantly induced by feeding with Glc, Fru, and Suc (*SI Appendix*, Fig. S10 *A* and *B*). The finding was further confirmed by the observed positive responses of *MdTST1* and *MdTST2* promoter activities to sugar feeding in tobacco leaves transiently expressing *MdTST1P-GUS* or *MdTST2P-GUS* reporter genes (Fig. 6 *A* and *B*), consistent with up-regulation of TSTs by sugars as previously reported (8). To further test the influence of *MdERDL6-1* expression on the transcription of *MdTST1* and *MdTST2*,35S:*MdERDL6-1* was transiently coexpressed with *MdTST1P: GUS* and/or *MdTST2P:GUS* in tobacco leaves. The analyses revealed that coexpression of *MdERDL6-1* increased the promoter activities of *MdTST1* and/or *MdTST2* (Fig. 6 *C* and *D*).

To determine the role of *MdTST1* and *MdTST2* in controlling sugar concentrations, we obtained overexpressing and silencing apple calli lines of *MdTST1* and *MdTST2*, respectively (*SI Appendix*, Fig. S11). Compared with the WT, the overexpression lines of *MdTST1* (OT1-1 and OT1-2) and *MdTST2* (OT2-1 and OT2-2) accelerated the growth of calli, whereas the silencing lines (ST1-1 and ST1-2 for *MdTST1*; ST2-1 and ST2-2 for *MdTST2*)

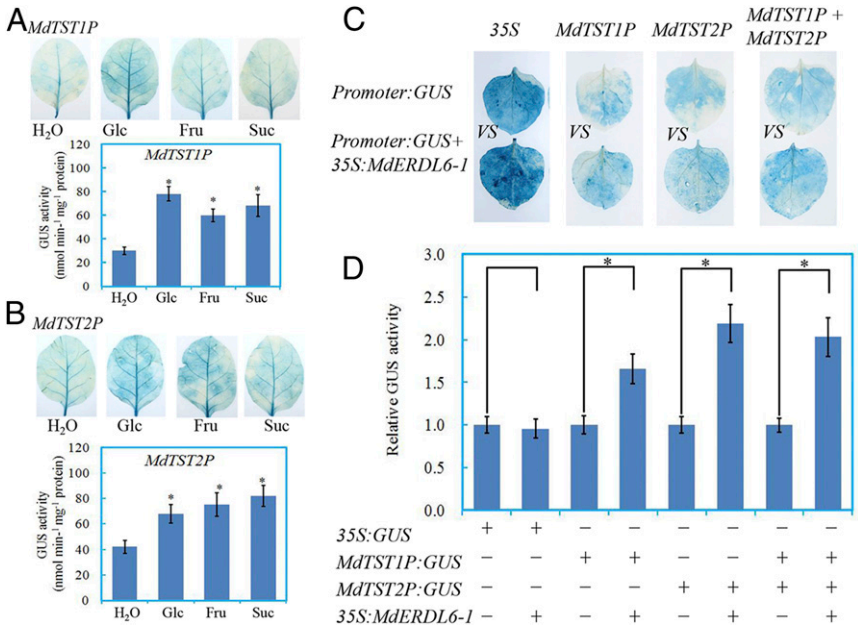

Fig. 6. The influence of sugar feeding and coexpression of 35S:*MdERDL6-1* on the promoter activities *of MdTST1* (*MdTST1P*) and *MdTST2* (*MdTST2P*). (*A* and *B*) The impact of sugar feeding on *MdTST1* (*A*) and *MdTST2* (*B*) promoter activities. Tobacco leaves were fed for 24 h with 2% different exogenous sugar, starting from 48 h after infiltrating with *Agrobacterium* harboring *MdTST1P* or *MdTST2P* plasmids. The treated and control leaves were harvested for GUS activity assay after 24 h feeding. (*C*) The impact of 35S:*MdERDL6-1* coexpression on *MdTST1* and *MdTST2* promoter activities. The 35S:GUS infiltration was used as a positive control. (*D*) The relative GUS activities of different combinations of infiltration. The treated leaves were harvested for GUS activity assay at 2 d after infiltration. "+" and "−" represent the presence or absence, respectively, of the *Agrobacterium* containing corresponding plasmids in the mixture for infiltration. The bars represent the mean value ± SD ($n \geq 4$). *$P \leq 0.05$, a significant difference from control.

inhibited calli growth (*SI Appendix*, Fig. S11*B*), as observed for *MdERDL6-1* transgenic calli (Fig. 3*B*). The *MdTST1* overexpression lines exhibited significantly increased Glc level in the transgenic calli, with moderate increases in Fru and Suc concentrations. Opposing results for the sugar concentration were detected in the silencing calli lines of *MdTST1* (*SI Appendix*, Fig. S11*C*). For *MdTST2* overexpressed lines, Fru and Suc levels were also significantly increased with only slight effect on Glc, while the silencing lines displayed reduced Fru and Suc levels (*SI Appendix*, Fig. S11*D*), supporting the theory that *MdTST2* played a more important role in controlling the accumulation of Fru and Suc than Glc in apple cells. Increased concentrations of the three soluble sugars in *MdTST1*- and *MdTST2*-overexpressing fruit calli concur with the notions that elevated sugar concentrations in *MdERDL6-1*–overexpressing apple calli and leaves are likely related to increased expression of *MdTST1* and *MdTST2*.

Up-Regulation of *SlTST1* and *SlTST2* Was Required for Elevating Sugar Concentrations in Tomatoes Expressing *MdERDL6-1*. To genetically determine whether the positive effect of *MdERDL6-1* on sugar levels is dependent on *TST1* and *TST2* expression, we generated *sltst1/2* double mutant in tomato using the CRISPR-Cas9 method, targeting the 5′ end of the *SlTST1* and *SlTST2* coding sequences. After sequencing verification, we obtained edited single and double mutant lines for *SlTST1* and *SlTST2* in the wild type background, where a series frame shifts of the target genes occurred (*SI Appendix*, Fig. S12*A*).

The single mutant lines for *SlTST1* (tst1-1 and -7) and *SlTST2* (tst2-6 and -13) exhibited no, or a slight but significant, decrease in hexoses and Suc concentrations, respectively, in the mature tomato fruits (*SI Appendix*, Fig. S12*B*) and leaves (*SI Appendix*, Fig. S13). The double mutant lines (tst1/2-4 and tst1/2-15) for *SlTST1* and *SlTST2* displayed much stronger reductions in the concentrations of the three soluble sugars than that in the single mutants (*SI Appendix*, Figs. S12*B* and S13). These results showed that there was a functional complementarity between *SlTST1* and *SlTST2* in modulating sugar accumulation in tomato, and *SlTST2* appears to play a more important role. Significantly, for the double mutant lines in the *MdERDL6-1* overexpressed background (OEs1-tst1/2-1 and OEs1-tst1/2-4), the concentrations of fruit Fru and Suc failed to be increased and remained at the same levels as that of *SlTST1* and *SlTST2* double mutant lines, whereas the concentration of Glc was lower than double mutant lines (Fig. 7), consistent with MdERDL6-1 acting as a vacuolar H^+/Glc exporter (Figs. 2 and 3). Similar phenomenon was observed in tomato leaves (*SI Appendix*, Fig. S13), indicating the conserved response between tomato fruits and leaves.

To gain further evidence if the dramatically increased sugar levels in the *MdERDL6-1* overexpressing lines (Figs. 4 and 7) are dependent on a high expression of *TST1* and *TST2*, we generated RNAi tomato lines with decreased expression levels of *SlTST1* and *SlTST2* by using virus-induced gene silencing (VIGS). Here, silencing of *SlTST1* and *SlTST2* in the WT tomato fruit reduced Glc, Fru, and Suc levels (*SI Appendix*, Fig. S14), confirming the role of *SlTSTs* in sugar import to the vacuoles (7–9 and *SI Appendix*, Figs. S12 and S13). A noteworthy observation is that in the *MdERDL6-1* overexpression lines (OEs-1 and -2), silencing of *SlTST1* and *SlTST2* by ∼65% to ∼70% (OEs1-TRV #4, OEs2-TRV#5) led to a ∼30% and ∼20% reduction in fruit hexoses and sucrose levels, respectively, in comparison with that in the *MdERDL6-1* overexpression controls, whereas a mild decrease of *SlTST1* and *SlTST2* mRNA levels by less than 10% (OEs1-TRV#1 and OEs2-TRV#2) did not reduce sugar levels in the overexpression background (*SI Appendix*, Fig. S14). This observation, together with the finding that the CRISPR-Cas9-mediated knockout of *SlTST1* and *SlTST2* decreased the sugar level further below the WT level in the *MdERDL6-1* overexpression background (Fig. 7 and *SI Appendix*, Fig. S12), indicates that the positive role of *MdERDL6-1* in sugar accumulation

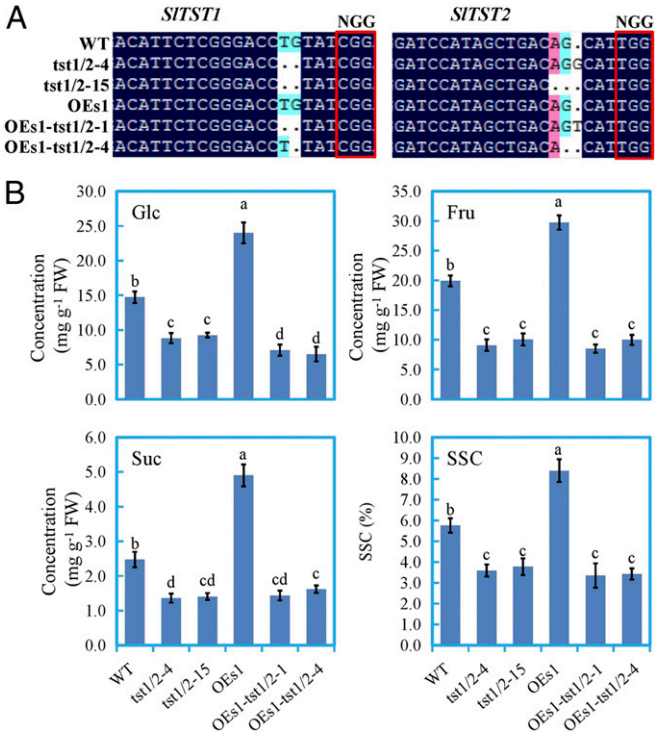

Fig. 7. CRISPR-Cas9–mediated knockout of *SlTST1* and *SlTST2* abolished the positive effect on sugar levels exerted by *MdERDL6-1* overexpression in tomato fruits. (*A*) The DNA sequence of the target region. *SlTST1* and *SlTST2* target sequences were chosen from CRISPR direct for gene editing. Sequences were aligned using DNAMAN. The dark region is the target sequence, and the other colored region is the difference in sequence among the lines indicated; the target sequences of WT and OEs-1 (transgenic line overexpressing MdERDL6-1) were the same as the control. The edited lines tst1/2-4 had two bases missing for *SlTST1* and one base inserted for *SlTST2*, while the tst1/2-15 had two bases missing for *SlTST1* and two bases missing for *SlTST2*. The OEs-1-tst1/2-1 had two bases missing for *SlTST1* and one base inserted for *SlTST2*, whereas the OEs-1-tst1/2-4 had one base missing for each of *SlTST1* and *SlTST2*. (*B*) The Glc, Fru, and Suc concentrations and soluble solids content in ripening fruit. The bars represent the mean value ± SD ($n \geq 4$). Different letters indicate significant differences at $P \leq 0.05$.

is achieved through *MdTST1* and *MdTST2* in apple or their orthologous genes, *SlTST1* and *SlTST2*, in tomato.

Discussion

Functional characterization of sugar transporters has mostly been performed in model plants, such as *Arabidopsis* and rice (7, 18, 30), where soluble sugar levels are low and rarely exceed 10 mM (31). Much less is known about roles of those transporters in organs that accumulate sugars to high concentrations, often more than 200 mM, such as in the mature fruits of apples (24), tomatoes (32), and watermelons (16). There is also a scarcity in understanding how different groups of transporters may work together to regulate growth and sugar homeostasis. Findings from the present work provide insight into the coordinated action of two classes of tonoplast sugar transporters that drives the accumulation of soluble sugar to high levels in apple and tomatoes.

MdERDL6-1, an Ortholog of AtERDL6, Encodes a Proton-Coupled Vacuolar Glc Exporter. In this study, we identified MdERDL6-1 from apples that shares a high sequence identity with AtERDL6 in *Arabidopsis* and BvIMP from sugar beets, both of which encode H^+/Glc symporters, delivering Glc to the cytosol from the vacuole (18, 19). Consistently, MdERDL6-1 was characterized in the yeast system as a proton-coupled Glc symporter with a K_m of 21.7 mM (Fig. 2 *D*–*F*). This K_m value is higher than that of many sugar transporters reported from other species (33) but comparable with that of LeHT1 and LeHT2, two H^+/hexose carriers in tomato fruit (21) and VvERDL6-13, a H^+/Suc symporters isolated from grape berries (34). In apple fruits, Glc in the vacuoles could reach over 100 mM. Thus, sugar transporters such as MdERDL6-1 with high K_m and V_{max} values appear to be commensurate with the physiological context to transport sugars from the vacuole to cytosol during fruit development.

Further evidence on MdERDL6-1 functioning as a proton-coupled tonoplast Glc exporter comes from transgenic analyses. First, silencing of *MdERDL6-1* in apple fruit calli significantly increased the Glc concentration (Fig. 3 *C* and *D*). This observation is consistent with that reported for the corresponding *erdl6* mutant of *Arabidopsis* exhibiting high Glc level in the vacuole (18, 19). Second, in the transgenic apples and tomatoes overexpressing *MdERDL6-1,* the down-regulated expression of *MdCAB1-1* and *SlCAB1* indicates an increased concentration of Glc in the cytosol of the transgenic lines (*SI Appendix*, Fig. S7), since *CAB1* expression is negatively controlled by the cytosolic Glc concentration (19). Third, all homologous genes encoding Glc-6-phosphate transporter 2, ADP-Glc pyrophosphorylase 3, and beta-amylase 3, that displayed a positive response to increased Glc in cytosol (35), were significantly up-regulated in the transgenic apple leaves overexpressing *MdERDL6-1* (Fig. 5*B*). Collectively, these findings indicate that more Glc was exported into cytosol from vacuole in transgenic apples and tomatoes overexpressing *MdERDL6-1*, further supporting the conclusion that MdERDL6-1 functions as a vacuolar Glc exporter.

Overexpression of *MdERDL6-1* Up-Regulated the Expression of *TST1/2*, Leading to an Increased Sugar Concentration in Apples and Tomatoes. One remarkable observation from this study is that overexpression of *MdERDL6-1* did not meet our expectation of decreasing Glc concentration in apple fruit calli and leaves and tomato fruits, as reported in transgenic *Arabidopsis* overexpressing a homolog of *AtERDL6*, *BvIMP* (19). On the contrary, it substantially increased the Glc, Fru, and Suc concentrations (Figs. 3 and 4), most likely stored in vacuoles that occupies the bulk of the cell volume (36).

Dynamic sugar storage in plant vacuoles is highly regulated by the balance between the import and export of sugars across tonoplast, mediated by different tonoplast sugar transporters (6). Among the DEGs identified from the *MdERDL6-1*-overexpressed lines, expression levels of *TST1* and *TST2*, homologous to *AtTMT1* and *AtTMT2* encoding tonoplast H^+/sugar antiporters in *Arabidopsis* (8, 9), were significantly up-regulated, resulting in an increased protein abundance for MdTST1 and 2 in apple leaves, and SlTST1 and 2 in tomato fruits (Fig. 5 and *SI Appendix*, Fig. S4). The expression of *AtTMT1* and *AtTMT2* is known to be strongly induced by Glc and with the latter also induced by Fru and Suc (8). Consistently, the promoter activities of *MdTST1* and *2* were indeed significantly enhanced by sugar feeding (Fig. 6 *A* and *B*). Further, CRISPR-Cas9–mediated knockout or VIGS-induced suppression of *SlTST1* and *2* in the *MdERDL6-1* overexpressed tomato lines blocked or reduced, respectively, the increase in sugar levels in mature fruits (Fig. 7 and *SI Appendix*, Fig. S14). Collectively, these findings demonstrate that the enhanced Glc efflux to cytosol by overexpressing *MdERDL6-1* up-regulates the expression of *TST1* and *TST2*, leading to accumulation of sugars in the vacuoles in apples and tomatoes.

Synchronizing Sugar Efflux and Influx across Tonoplasts Mediated by ERDL6 and TSTs Controls Intracellular Sugar Homeostasis. As discussed above, the transgenic lines overexpressing *MdERDL6-1*

likely exported more Glc into the cytoplasm to induce or enhance the expression of *TST1* and *TST2* to import sugars to the vacuoles in the *MdERDL6-1*–overexpressing plants (Figs. 4–7), a view also supported by the coexpression patterns of *MdERDL6-1*, *MdTST1*, and *MdTST2* in developmental fruit of apple (Fig. 1). As with many other fleshy fruits, Suc, Fru, and Glc are stored in the central vacuoles of parenchyma cells in apple and tomato fruit pericarps, with their collective concentration reaching 300 to ~400 mM at maturity (36), which is far more than that in other tissues, such as leaves (32, 37). It remains unclear how such a high level of soluble sugars could be accumulated in the vacuole from the cytosol, apart from vacuolar lumen in most fruit cells are highly acidic (38), hence favoring the activities of tonoplast H^+/sugar antiporters. Our findings on the regulation of *TST1/2* expression by *MdERDL6-1* reveal a mechanism of regulating sugar status between the cytosol and vacuole.

Biochemical and evolutionary studies have established that cytosolic sugar homeostasis is critical for fundamental cellular function and needs to be tightly controlled at an optimum level (1, 39). We hypothesize that an increase in the Glc level in the cytosol would trigger an influx system to transport sugars to the vacuole, thereby maintaining sugar homeostasis in the cytoplasm. It is probably an effective and advantageous strategy to channel physiologically excessive sugars to the vacuole rather than to other subcellular compartments when the cytosolic Glc levels or signals are above a threshold value. Here, for a given amount of Glc exported from the vacuole, its concentration in the cytoplasm might be instantaneously increased by nearly eightfold, assuming the vacuole occupies up to 80%, with the cytosol occupying 10% (half of the cytoplasm) of the cell volume (36). In this way, the *MdERDL6-1*–derived cytosolic Glc could act as an effective signal to up-regulate TSTs to import sugars into the vacuole from cytosol (Fig. 8). To this end, increased cytosolic sugar levels, indicated by a decreased *CAB1* expression, have been observed in *Arabidopsis* overexpressing *BvIMP* that encodes a tonoplast H^+/Glc symporter (19). On the other hand, the role of *AtTMT1* in importing sugars from the cytosol to the vacuole was shown by analyzing the *tmt1* knockout mutant upon feeding with Glc, Fru, or Suc (8). More recently, vernalization-induced sink-to-source transition of sugar beet root was linked with increased expression of *BvSUT4* but reduced expression of *BvTST2.1* for Suc export from and import into vacuoles, respectively (7). In both cases, however, it was unknown if the tonoplast sugar exporters and importers were modulated by one or another.

The cytosolic sugar homeostasis is regulated by multiple metabolic and transport processes (1). Thus, it is not surprising that there are a number of sugar-related DEGs in the apple leaves overexpressing *MdERDL6-1* (Fig. 5*A*). Here, in addition to the significant up-regulation of *MdTST1* and *2*, *MdSWEET2*, a homologous gene to *AtSWEET2* for exporting Glc from vacuole to cytosol in *Arabidopsis* roots (40), was down-regulated (Fig. 5*A*), probably to avoid further rise of Glc level in the cytosol due to *MdERDL6-1* overexpression. Interestingly, several predicted plasma membrane sugar transporter genes were also down-regulated in response to *MdERDL6-1* overexpression. These include one *MdSUC1* gene for Suc and three *MdHT* genes for Glc or Fru, as well as five *MdSOT* genes for sorbitol (Fig. 5*A*). We speculate that the down-regulation of these transporter genes may potentially contribute to the rebalancing of sugar homeostasis in the cytosol by reducing sugar import from extracellular space. It is also worth noting that genes for two cell wall invertases, one cytosolic invertase and three sucrose synthases were also down-regulated (Fig. 5*A*). This indicates a reduced sucrose cleavage in the cells overexpressing *MdERDL6-1*, likely to help alleviating the elevation of cytosolic Glc levels. Pertinently, a coordinated regulation between some plasma membrane sugar transporter and cell wall invertase genes has been

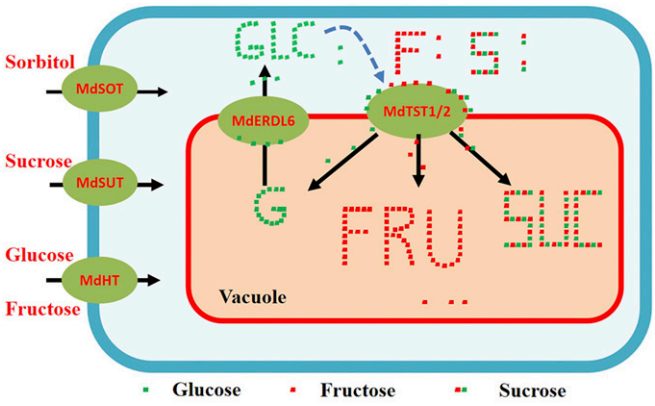

Fig. 8. A model on how *MdERDL6* could modulate sugar accumulation in vacuole through regulating *MdTST1/2* or their orthologous genes. In apple fruits, sugars are unloaded from the phloem into the parenchyma cells via transporters MdSUT, MdHT, and MdSOT for sucrose, hexose, and sorbitol, respectively. Upon meeting the requirements for energy and carbon skeleton production, excessive soluble sugars are imported into the vacuoles for storage, mediated by a set of tonoplast sugar transporters including the H^+/sugar antiporters, MdTST1 and MdTST2. On the other hand, MdERDL6-1 acts as an H^+/sugar symporter to export glucose from the vacuole to cytosol. Findings from our study indicate that the MdERDL6-mediated glucose efflux to the cytosol activates or enhances the expression of *MdTST1* and *MdTST2* to import sugars into the vacuole, leading to the accumulation of high concentration of sugars. Our data also indicate that the model is likely applicable to other systems such as tomato fruits (see article text for details). G/Glc, glucose; F/Fru, fructose; S/Suc, sucrose.

recently reported in apple and tomato fruits (4, 41) and *Arabidopsis* floral organs (42).

Overexpression of *MdERDL6-1* under the 35S promoter might result in too much Glc to be exported by the H^+/Glc symporter to the cytosol, thereby generating an unusual situation affecting expression of TSTs. This scenario is unlikely, since there was only 40 to 60% reduction in the transcript level of *CAB1* in apple leaves, tomato leaves, and fruits (*SI Appendix*, Fig. S7). Such a level of changes in *CAB1* transcripts is within the range observed during plant development and in response to environmental changes (8, 19, 29), indicating that the increased cytosolic Glc from the *MdERDL6-1*-overexpressed plants is within the physiological levels. The two- to fourfold increase in MdTST1/2 and SlTST1/2 abundance in the transgenic apple and tomato (Fig. 5 *E* and *G* and *SI Appendix*, Fig. S4) also falls in range of fluctuation in protein levels during plant growth and development. Consistent with this view is the normal growth of the apple seedlings overexpressing *MdERDL6-1* (*SI Appendix*, Fig. S3*A*). Heterologous expression of *MdERDL6-1* in tomato promoted vegetative growth and generated fertile plants but delayed flowerings and reduced seed and fruit number (*SI Appendix*, Fig. S3*E* and Table S2). The latter finding indicates that reproductive development is sensitive to the MdERDL6-1–induced rise of cytosolic Glc level, consistent with the critical role of sugar signaling in ovule initiation and seed set, as recently shown in *Arabidopsis* (42). Collectively, the data indicates 1) the up-regulation of *TST1/2* expression by MdERDL6-1-mediated Glc efflux likely occur *in planta* and 2) the abnormal flowering and seed set observed in the *MdERDL6-1* overexpression tomato lines under the CaMV35S promoter is probably due to misexpression of the transgene in cellular sites that otherwise show no or little *ERDL6* expression or the up-regulation of the *SlTSTs* is not sufficient to counteract the increased efflux of Glc from vacuole to cytosol in the reproductive organs.

In summary, we showed in this study that MdERDL6-1 encodes a tonoplast H^+/sugar symporter to export Glc from the vacuole to cytosol. Significantly, overexpression of *MdERDL6-1*

substantially increased the Suc, Fru, and Glc levels in apple fruit calli and leaves, and tomato fruits and leaves, which was due to the up-regulation of the expression of the H^+/sugar antiporter genes, *TST1* and *TST2*. The finding offers insight into the regulatory mechanism of sugar accumulation, in which an increased cytoplasmic Glc level mediated by MdERDL6 activates the expression of *TST1* and *TST2* to import sugars into the vacuole, probably through sugar signaling effect of Glc (Fig. 8). High expression of homologous *ERDL6* genes has also been observed in fruits of many other species, such as pineapple (20) and orange (22), indicating the ERDL6-regualted vacuolar sugar accumulation pathway (Fig. 8) may operate in a broad range of fruit crops. It remains to be determined as how the cytoplasmic Glc signals are sensed and transmitted to modulate the expression of *TST1* and *TST2* and if the high expression trait of *ERDL6-TST* nexus was selected during evolution and domestication of fruit crops.

Materials and Methods

Plant Materials. The samples from the "Gala" apple (*Malus domestica*) were the same as those used in our previous report (23). Fruits were sampled between 3:00 PM and 4:00 PM at 16, 34, 55, 75, 98, and 122 (maturity) days after bloom (DAB), corresponding to the timing of major physiological events for "Gala" fruit (24). On each collection date, six apples per replicate were harvested from three trees, with five replicates in total. The fruits were immediately weighed, cut into small pieces after the core was removed, and frozen on-site in liquid nitrogen. Additionally, full flowers, roots, mature leaves, and shoot tips were also collected. All frozen samples were stored at –80 °C until use.

Tissue-cultured WT and *MdERDL6-1*–transformed "GL3" apple plantlets were initially grown on Murashige and Skoog (MS) medium supplemented with 25 mg · L^{-1} kanamycin, 0.2 mg · L^{-1} IAA, and 0.3 mg · L^{-1} 6-BA for 4 wk. They were then transferred to a rooting MS medium supplemented with 0.5 mg · L^{-1} IAA and 0.5 mg · L^{-1} IBA. After rooting, plants of both genotypes were transferred to a culture room maintained at 23 °C with a 14-h photoperiod, supplemented with fluorescent light (60 μmol · m^{-2} · s^{-1}). After these plants had grown for three months, the fourth to eighth leaves from the base of the stem (fully mature leaves) were sampled. The samples were immediately frozen in liquid nitrogen and stored at –80 °C for further analysis.

Phylogenetic Identification of the *MdERDL6* Genes. Candidate genes were identified by performing a BLASTp (protein-protein BLAST) analysis against the apple gene set (amino acids) in the *Malus* × *domestica* genome, GDDH13 v1.1 (25). As a query, we used sequences for *Arabidopsis* ERDL6, TST, and vGT obtained from The *Arabidopsis* Information Resource. An E-value of 1.00E-10 was set as the threshold. Putative candidate gene sequences were retrieved from the *Malus* genome GDDH13 v1.1. We then constructed neighbor-joining phylogenetic trees with 1,000 trials of bootstrap replicates using MEGA 6.

RNA-Seq and Data Analysis. RNA-seq data were generated from a "greensleeves" apple fruit taken at five developmental stages (16, 41, 70, 94, and 128 DAB) and recently fully expanded leaves, with three biological replicates, to determine the expression patterns of the apple sugar transporter genes, as reported by Li et al. (24). Sequencing was performed using an Illumina HiSEq. 2000 sequencer with 50-base-pair (bp) single-end sequencing (Illumina, San Diego, CA) in 2012. However, RNA-seq for transgenic apple leaves in 2017 was sequenced using an Illumina HiSEq 2500 sequencer with 250-bp single-end sequencing (Illumina, San Diego, CA) at Biomarker Technologies, China.

The RNA-seq reads were processed by removing barcode and adaptor sequences first, followed by alignments to the rRNA database Silva using Bowtie, allowing up to three mismatches to remove potential contaminating reads. The clean reads were then aligned to the *Malus* Genome GDDH13 Version 1.1 (25) using Tophat, allowing one mismatch. After alignment, raw counts of mapped reads for each *Malus* gene model of GDDH13 Version 1.1 were derived and then normalized to the RPKM per million mapped reads .

Gene Cloning and Subcellular Localization. Total RNA was extracted from "gala" fruit by using the cetyl trimethyl ammonium bromide method. A set of specific primers (*SI Appendix*, Table S1) were used to clone the complementary DNAs (cDNAs) of *MdERDL6-1*, *MdTST1,* and *MdTST2*.

To determine its subcellular localization, the full-length open reading frame (ORF) of *MdERDL6-1* without the stop codon was cloned into the pMDC83-GFP vector under the control of the CaMV35S promoter, and GFP was attached to the C terminus of the target gene. To examine transient expression, we transformed both the *MdERDL6-1* fusion plasmid and tonoplast targeting vector VAC-RK (vacuole marker) CD3–975 into *Arabidopsis* mesophyll protoplasts and apple calli protoplasts via polyethylene glycol-mediated transformation (43, 44). Furthermore, we also isolated the vacuoles of *N. benthamiana* leaves, which were infiltrated with *Agrobacterium tumefaciens* containing MdERDL6-1-GFP plasmid for 3 d, as described in (45), with minor modifications. The isolated protoplasts and vacuoles were examined for GFP signal and chlorophyll autofluorescence using a confocal laser-scanning microscope (LSM 710; Carl Zeiss) at excitation wavelengths of 488 nm for GFP and 633 nm for chlorophyll autofluorescence.

Heterologous Expression of *MdERDL6-1* in Yeast. To determine the subcellular localization of *MdERDL6-1* in yeast, we amplified the full-length ORF of *MdERDL6-1* without the stop codon into the pYES-DEST2-eGFP vector for transformation into the hexose transporter-deficient yeast strain EBY.VW4000, which grows only on maltose (26). The GFP fluorescence of the transformed yeast was visualized under a fluorescence microscope (x 600 to 800 nm) (LSM 710; Carl Zeiss).

To determine the sugar transport properties of MdERDL6-1, its ORF was inserted into the pYES-DEST2 vector and transferred into the yeast strain EBY.VW4000 (26). For uptake experiments with ^{14}C-labeled sugars to test H^+/sugar symport across plasma membrane in yeast, single colonies of yeast strain EBY.VW4000, containing pYES-DEST2-MdERDL6-1 or empty pYES-DEST2 vector, were precultured on maltose-casamino acid medium (0.67% weight (wt)/volume yeast nitrogen base, 1% wt/volume casamino acids, 0.002% wt/volume Trp, and 2% wt/volume maltose) to an OD_{600} value of 0.8. The transport assay was then performed as described by Sauer and Stadler (46). For the inhibitor assays, a final concentration of 50-μM CCCP, as a proton uncoupler, was added to energized yeast cells 30 s before the addition of ^{14}C-labeled Glc.

Vector Constructs and Apple Transformation. To construct the vectors for overexpression of *MdERDL6-1*, *MdTST1*, and *MdTST2*, we introduced the respective coding sequence into the pGWB402 binary vector under the CaMV35S promoter. The RNAi constructs were generated using the RNAi vector, pHannibal, and the binary vector, pCAMBIA2300. The specific PCR fragments of the target genes (*MdERDL6-1*: 301 bp, *MdTST1*: 313 bp, and *MdTST2*: 311 bp) were inserted into the pHannibal vector in antisense orientation. The pHannibal vectors containing target fragments were then subcloned into the binary vector, pCAMBIA2300. The recombinant plasmids were introduced into the *Agrobacterium tumefaciens* strain, EHA105.

Transgenic apple plants were generated from leaf fragments through *Agrobacterium*-mediated transformation, as previously described (38). Regenerated Kan-resistant buds were subcultured every 3 wk. The candidate resistant lines were subcultured every 4 wk and rooted using the two-phase method following the description of Dai et al. (47). A total of 25 rooting plants were grown in a greenhouse for at least 2 mo. *MdERDL6-1* expression in mature leaves from three independently transformed lines was detected by qRT-PCR and Western blotting. Respective samples harvested were used for measurement of sugar concentrations and RNA-seq with at least three biological replications in each case.

Tomato Transformation. The pGWB402-MdERDL6-1 construct was transformed into tomato (*Solanum lycopersicum* cv. Micro-Tom), as previously described (48). Tomato plants were grown at 25 °C with a 16-h photoperiod, supplemented with light at 120 μmol m^{-2} s^{-1}. The transgenic lines were screened by Kan resistance and PCR analysis with homozygous lines identified at T3 generation.

For the CRISPR-Cas9 experiment, the target sequences for *SlTST1* and *SlTST2* were designed using CRISPR direct (http://crispr.dbcls.jp/), and the sequence specificity was confirmed by BLAST in National Center for Biotechnology Information. After the specificity was verified in Micro-Tom tomatoes, the target sequence was synthesized and cloned into the pHSE401 vector to construct the single target vector for *SlTST1* or *SlTST2,* as described by Xing et al. (49). Moreover, a double target vector against *SlTST1* and *SlTST2* was produced. The single target vector for *SlTST1* or *SlTST2* was transformed into WT Micro-Tom tomatoes to identify their respective functions in controlling sugar concentration in tomato, while the double target vector was transformed into WT Micro-Tom tomatoes and the transgenic tomato line overexpressing *MdERDL6-1*. Following transformation, the edited lines were screened by hygromycin resistance and sequencing.

Virus-Induced Gene Silencing of *SlTST1/2* in Tomato Fruits. Specific partial sequences of *SlTST1* (290 bp) and *SlTST2* (285 bp) were cloned from tomato leaves using RT-PCR. The resulting PCR products were both inserted into the pTRV2 (tobacco rattle virus) vector in tandem under the control of the dual CaMV35S promoter. Then, the *Agrobacterium* strain EHA105 contained the resulting vector pTRV2-SlTST1/2 and pTRV1 were cultured to OD_{600} of around 1.0 respectively, and resuspended to OD_{600} of 0.4 to 0.6 at a 1:1 ratio with pTRV1 (with empty pTRV2 as a control), which were used for infiltration of the carpopodium of tomato fruit, attached to the plant by *Agrobacterium*-mediated transformation, as described previously (50). Ten days after infiltration, the tomato fruit were harvested for quantification of *SlTST1* and *SlTST2*, and measurement of sugar concentrations.

Measurements of Soluble Sugars, Starch, and CO_2 Assimilation Rate. Soluble sugars and sorbitol were extracted and derivatized sequentially with methoxyamine hydrochloride and *N*-methyl-*N*-trimethylsilyl-trifluoroacetamide, as previously described (51). Thereafter, the metabolites were analyzed with a Shimadzu GCMS-2010SE (Shimadzu Corporation, Kyoto, Japan). The tissue residue that remained after 75% methanol extraction for gas chromatography-mass spectrometry (GC–MS) analysis was re-extracted three times with 80% (volume/volume) ethanol at 80 °C, and the pellet was retained for starch determinations (23). Additionally, the assimilation of CO_2 in seedling leaves was monitored between 9:30 and 11:30 AM, using a LI-COR 6400 portable photosynthesis system (LI-COR, Huntington Beach, CA).

Analysis of mRNA Expression. qRT-PCR was used to analyze the expression of all detected genes. After sequence similarities were examined based on *Malus domestica* or *Solanum lycopersicum* genome data, gene-specific primers (*SI Appendix*, Table S1) were designed using Primer 5 software. Primer specificity was determined by RT-PCR and melting curve analysis. qRT-PCR was performed on an ABI7300 Real-Time PCR System (Thermo Fisher Scientific). Transcripts of *Actin* (GenBank: CN938023 for apple, and BT013707 for tomato) served to standardize the cDNA from our test genes. For each sample, total RNA was extracted from three biological replicates before the qRT-PCR experiments were run. All data were examined by the delta-delta cycle threshold (ddCT) method.

Promoter Cloning and Analysis of Activity. To examine why *MdTST1* and *MdTST2* expression were up-regulated in the transgenic plants overexpressing *MdERDL6-1*, we designed primers to clone the promoters of *MdTST1* and *MdTST2* based on their genome sequences (*SI Appendix*, Table S1). About 1.8 kb of DNA sequence, upstream of *MdTST1* or *MdTST2* mRNA, was cloned from the genomic DNA of the "Royal Gala" apple. To examine transient gene expression in tobacco, the *MdTST1* and *MdTST2* promoters were introduced into the pC0390GUS vector to generate *MdTST1P:GUS* and *MdTST2P:GUS*. The p35S:GUS vector and the empty vector pC0390GUS were used as the positive and negative controls, respectively. *Agrobacterium*-mediated transient transformation was carried out on unfolded leaves according to the protocol previously described (52). Exogenous sugar feeding was conducted on tobacco leaves 48 h following agroinfiltration. Here, tobacco leaves were cut at the petioles and immediately inserted into different 2% sugar solutions or water for 24 h before being harvested for measurement of β-glucuronidase (GUS) activity.

To test whether *MdERDL6-1* could regulate the expression of *MdTST1* and *MdTST2*, we investigate the influence of *MdERDL6-1* expression on activities of *MdTST1* and *MdTST2* promoters via transient coexpression of 35S:*MdERDL6-1* and *MdTST1P:GUS,* and/or *MdTST2P:GUS,* in tobacco leaves. The leaves were sampled to measure GUS activity 48 h after the infiltration.

Western Blotting. Total protein samples were extracted from apple leaves and tomato fruits as previously described (53), and the total concentrations were determined with protein assay kits (Bio-Rad, Hercules, CA) using bovine serum albumin as a standard. Specific monoclonal antibodies were raised in rabbits (Genscript, Nanjing, China) against a peptide from a highly conserved region in MdERDL6-1 (GSLSNVGAMVGAIAS), MdTST1 (FYLPESPRWLVSKGR, conserved sequences with SlTST1), and MdTST2 (VEGLIVAMSLIGAT, conserved sequences with SlTST2), respectively. Actin abundance was monitored with a monoclonal antibody (CWBIO, Beijing, China). The antigen-antibody complexes were detected using Clarity Western ECL Substrate (Bio-Rad, Hercules, CA), and the protein bands of Western blotting were quantified using Image J software according to the manufacturer's instructions.

Statistical Analysis. All data were analyzed via IBM SPSS Statistics 21 and graphed with Sigma Plot 10.0 software. Data were analyzed using independent *t* tests or one-way ANOVA tests, with a significance level accepted at $P < 0.05$.

Data Availability. All study data are included in the article and supporting information.

ACKNOWLEDGMENTS. This work was supported by the Program for the National Key Research and Development Program (2018YFD1000200), the National Natural Science Foundation of China (No. 31872043), the Training Program Foundation for the Young Talents of Northwest A&F University to M.L., and Australian Research Council (DP180103834) to Y.-L.R.

1. Y.-L. Ruan, Sucrose metabolism: Gateway to diverse carbon use and sugar signaling. *Annu. Rev. Plant Biol.* **65**, 33–67 (2014).
2. J. W. Patrick, F. C. Botha, R. G. Birch, Metabolic engineering of sugars and simple sugar derivatives in plants. *Plant Biotechnol. J.* **11**, 142–156 (2013).
3. Y.-L. Ruan, J. W. Patrick, H. Weber, Assimilate partitioning and plant development. *Mol. Plant* **3**, 941 (2010).
4. Z. Wang *et al*., Heterologous expression of the apple hexose transporter MdHT2.2 altered sugar concentration with increasing cell wall invertase activity in tomato fruit. *Plant Biotechnol. J.* **18**, 540–552 (2020).
5. E. Martinoia, Vacuolar transporters–Companions on a longtime journey. *Plant Physiol.* **176**, 1384–1407 (2018).
6. R. Hedrich, N. Sauer, H. E. Neuhaus, Sugar transport across the plant vacuolar membrane: Nature and regulation of carrier proteins. *Curr. Opin. Plant Biol.* **25**, 63–70 (2015).
7. C. M. Rodrigues *et al*., Vernalization alters sink and source identities and reverses phloem translocation from taproots to shoots in sugar beet. *Plant Cell* **32**, 3206–3223 (2020).
8. A. Wormit *et al*., Molecular identification and physiological characterization of a novel monosaccharide transporter from *Arabidopsis* involved in vacuolar sugar transport. *Plant Cell* **18**, 3476–3490 (2006).
9. B. Jung *et al*., Identification of the transporter responsible for sucrose accumulation in sugar beet taproots. *Nat. Plants* **1**, 14001 (2015).
10. S. Aluri, M. Büttner, Identification and functional expression of the *Arabidopsis thaliana* vacuolar glucose transporter 1 and its role in seed germination and flowering. *Proc. Natl. Acad. Sci. U.S.A.* **104**, 2537–2542 (2007).
11. A. Schulz *et al*., Proton-driven sucrose symport and antiport are provided by the vacuolar transporters SUC4 and TMT1/2. *Plant J.* **68**, 129–136 (2011).
12. L. Q. Chen *et al*., Sugar transporters for intercellular exchange and nutrition of pathogens. *Nature* **468**, 527–532 (2010).
13. P. A. Klemens *et al*., Overexpression of the vacuolar sugar carrier AtSWEET16 modifies germination, growth, and stress tolerance in *Arabidopsis*. *Plant Physiol.* **163**, 1338–1352 (2013).
14. W. J. Guo *et al*., SWEET17, a facilitative transporter, mediates fructose transport across the tonoplast of *Arabidopsis* roots and leaves. *Plant Physiol.* **164**, 777–789 (2014).
15. J. Cheng *et al*., Overexpression of the tonoplast sugar transporter CmTST2 in melon fruit increases sugar accumulation. *J. Exp. Bot.* **69**, 511–523 (2018).
16. Y. Ren *et al*., A tonoplast sugar transporter underlies a sugar accumulation QTL in watermelon. *Plant Physiol.* **176**, 836–850 (2018).
17. S. Schneider *et al*., Vacuoles release sucrose via tonoplast-localised SUC4-type transporters. *Plant Biol.* **14**, 325–336 (2012).
18. G. Poschet *et al*., A novel *Arabidopsis* vacuolar glucose exporter is involved in cellular sugar homeostasis and affects the composition of seed storage compounds. *Plant Physiol.* **157**, 1664–1676 (2011).
19. P. A. Klemens *et al*., Overexpression of a proton-coupled vacuolar glucose exporter impairs freezing tolerance and seed germination. *New Phytol.* **202**, 188–197 (2014).
20. E. Antony *et al*., Cloning, localization and expression analysis of vacuolar sugar transporters in the CAM plant *Ananas comosus* (pineapple). *J. Exp. Bot.* **59**, 1895–1908 (2008).
21. D. W. McCurdy, S. Dibley, R. Cahyanegara, A. Martin, J. W. Patrick, Functional characterization and RNAi-mediated suppression reveals roles for hexose transporters in sugar accumulation by tomato fruit. *Mol. Plant* **3**, 1049–1063 (2010).
22. Q. Zheng, Z. Tang, Q. Xu, X. Deng, Isolation, phylogenetic relationship and expression profiling of sugar transporter genes in sweet orange (*Citrus sinensis*). *Plant Cell Tiss. Org. Cult.* **119**, 609–624 (2014).
23. X. Wei, F. Liu, C. Chen, F. Ma, M. Li, The *Malus domestica* sugar transporter gene family: Identifications based on genome and expression profiling related to the accumulation of fruit sugars. *Front Plant Sci* **5**, 569 (2014).
24. M. Li *et al*., Proteomic analysis reveals dynamic regulation of fruit development and sugar and acid accumulation in apple. *J. Exp. Bot.* **67**, 5145–5157 (2016).
25. N. Daccord *et al*., High-quality de novo assembly of the apple genome and methylome dynamics of early fruit development. *Nat. Genet.* **49**, 1099–1106 (2017).
26. R. Wieczorke *et al*., Concurrent knock-out of at least 20 transporter genes is required to block uptake of hexoses in *Saccharomyces cerevisiae*. *FEBS Lett.* **464**, 123–128 (1999).

27. X. B. Xie *et al*., The bHLH transcription factor MdbHLH3 promotes anthocyanin accumulation and fruit colouration in response to low temperature in apples. *Plant Cell Environ.* **35**, 1884–1897 (2012).
28. D. G. Hu *et al*., MdMYB1 regulates anthocyanin and malate accumulation by directly facilitating their transport into vacuoles in apples. *Plant Physiol.* **170**, 1315–1330 (2016).
29. K. E. Koch, Carbohydrate-modulated gene expression in plants. *Annu. Rev. Plant Physiol. Plant Mol. Biol.* **47**, 509–540 (1996).
30. S. N. Oliver, E. S. Dennis, R. Dolferus, ABA regulates apoplastic sugar transport and is a potential signal for cold-induced pollen sterility in rice. *Plant Cell Physiol.* **48**, 1319–1330 (2007).
31. T. L. Slewinski, Diverse functional roles of monosaccharide transporters and their homologs in vascular plants: A physiological perspective. *Mol. Plant* **4**, 641–662 (2011).
32. Y.-L. Ruan, J. W. Patrick, C. Brady, Protoplast hexose carrier activity is a determinate of genotypic difference in hexose storage in tomato fruit. *Plant Cell Environ.* **20**, 341–349 (1997).
33. M. Büttner, N. Sauer, Monosaccharide transporters in plants: Structure, function and physiology. *Biochim. Biophys. Acta* **1465**, 263–274 (2000).
34. R. Breia *et al*., VvERD6l13 is a grapevine sucrose transporter highly up-regulated in response to infection by *Botrytis cinerea* and *Erysiphe necator*. *Plant Physiol. Biochem.* **154**, 508–516 (2020).
35. Q. Chen *et al*., WRKY18 and WRKY53 coordinate with Histone Acetyltransferase1 to regulate rapid responses to sugar. *Plant Physiol.* **180**, 2212–2226 (2019).
36. S. Yamaki, Metabolism and accumulation of sugars translocated to fruit and their regulation. *J. Jpn. Soc. Hortic. Sci.* **79**, 1–15 (2010).
37. M. Li, F. Feng, L. Cheng, Expression patterns of genes involved in sugar metabolism and accumulation during apple fruit development. *PLoS One* **7**, e33055 (2012).
38. P. Strazzer *et al*., Hyperacidification of *Citrus* fruits by a vacuolar proton-pumping P-ATPase complex. *Nat. Commun.* **10**, 744 (2019).
39. H. Wan, L. Wu, Y. Yang, G. Zhou, Y. L. Ruan, Evolution of sucrose metabolism the dichotomy of invertases and beyond. *Trends Plant Sci.* **23**, 163–177 (2018).
40. H. Y. Chen *et al*., The *Arabidopsis* vacuolar sugar transporter SWEET2 limits carbon sequestration from roots and restricts *Pythium infection*. *Plant J.* **83**, 1046–1058 (2015).
41. L. Ru *et al*., Transcriptomic and metabolomics responses to elevated cell wall invertase activity during tomato fruit set. *J. Exp. Bot.* **68**, 4263–4279 (2017).
42. S. Liao, L. Wang, J. Li, Y.-L. Ruan, Cell wall invertase is essential for ovule development through sugar signaling rather than provision of carbon. *Plant Physiol.* **183**, 1126–1144 (2020).
43. S. D. Yoo, Y. H. Cho, J. Sheen, *Arabidopsis* mesophyll protoplasts: A versatile cell system for transient gene expression analysis. *Nat. Protoc.* **2**, 1565–1572 (2007).
44. H. Xu *et al*., MdMYB6 regulates anthocyanin formation in apple both through direct inhibition of the biosynthesis pathway and through substrate removal. *Hortic. Res.* **7**, 72 (2020).
45. C. Li *et al*., Apple ALMT9 requires a conserved C-terminal domain for malate transport underlying fruit acidity. *Plant Physiol.* **182**, 992–1006 (2020).
46. N. Sauer, R. Stadler, A sink-specific H^+/monosaccharide co-transporter from *Nicotiana tabacum*: Cloning and heterologous expression in baker's yeast. *Plant J.* **4**, 601–610 (1993).
47. H. Dai *et al*., Development of a seedling clone with high regeneration capacity and susceptibility to *Agrobacterium* in apple. *Sci. Hortic. (Amsterdam)* **164**, 202–208 (2013).
48. H. J. Sun, S. Uchii, S. Watanabe, H. Ezura, A highly efficient transformation protocol for Micro-Tom, a model cultivar for tomato functional genomics. *Plant Cell Physiol.* **47**, 426–431 (2006).
49. H. L. Xing *et al*., A CRISPR/Cas9 toolkit for multiplex genome editing in plants. *BMC Plant Biol.* **14**, 327 (2014).
50. D. Q. Fu, B. Z. Zhu, H. L. Zhu, W. B. Jiang, Y. B. Luo, Virus-induced gene silencing in tomato fruit. *Plant J.* **43**, 299–308 (2005).
51. M. Li, P. Li, F. Ma, A. M. Dandekar, L. Cheng, Sugar metabolism and accumulation in the fruit of transgenic apple trees with decreased sorbitol synthesis. *Hortic. Res.* **5**, 60 (2018).
52. I. A. Sparkes, J. Runions, A. Kearns, C. Hawes, Rapid, transient expression of fluorescent fusion proteins in tobacco plants and generation of stably transformed plants. *Nat. Protoc.* **1**, 2019–2025 (2006).
53. J. Yang *et al*., Increased activity of MdFRK2, a high-affinity fructokinase, leads to upregulation of sorbitol metabolism and downregulation of sucrose metabolism in apple leaves. *Hortic. Res.* **5**, 71 (2018).